Development of Pendant Drop Mechanical Analysis as a Technique for Determining the Stress–Relaxation and Water-Permeation Properties of Interfacially Polymerized Barrier Layers

Vivek P. Khare,[1] Alan R. Greenberg,[1] William B. Krantz[2]

[1]*Department of Mechanical Engineering, University of Colorado, Boulder, Colorado 80309-0427*
[2]*Department of Chemical and Materials Engineering, University of Cincinnati, Cincinnati, Ohio 45221-0012*

Received 18 October 2002; accepted 6 March 2003

ABSTRACT: Interfacial polymerization (IP) involves the formation of solid polymeric films at the interface between aqueous and immiscible organic solutions via an interfacial polycondensation reaction between complementary monomeric reactants present in the two solutions. IP films are very thin (<0.25 μm) and form effective barrier layers in interfacially polymerized thin-film composite membranes. Considerable difficulties are encountered in applying conventional characterization techniques to such unsupported IP thin films. This article describes the development of a novel technique, pendant drop mechanical analysis (PDMA), which can be used to study the mechanical and transport behavior of unsupported IP films. Experiments were conducted on films formed in a PDMA apparatus via the IP polymerization of *m*-phenylene diamine and trimesoyl chloride (TMC). Stress–relaxation data obtained via PDMA were fitted with the Williams–Watts equation, and the results indicated a statistically significant dependence of the model parameters on the TMC concentration. Permeation experiments also demonstrated a statistically significant dependence of the membrane constant on the TMC concentration. The results provide unique insights regarding the relationship between structure and performance in unsupported IP films and suggest that network formation is enhanced in a concentration range of 0.1–0.3 wt % TMC. Although refinements are required, PDMA appears to be a promising technique for identifying optimum IP reaction conditions and assessing corresponding mechanical and transport characteristics. © 2003 Wiley Periodicals, Inc. J Appl Polym Sci 90: 2618–2628, 2003

Key words: membranes; polyamides; mechanical properties; interfacial polymerization

INTRODUCTION

Thin-film composite (TFC) membranes consist of thin and dense barrier layers that provide permselective properties and much thicker porous substrates that provide mechanical support without adversely affecting the permeability. This approach offers great flexibility because the properties of the two layers can be manipulated independently to suit specific separation requirements.

Interfacial polymerization (IP) is a versatile technique that is used to form the TFC permselective layer. IP involves the formation of a solid polymeric film at the interface between aqueous and immiscible organic solutions, each of which contains a complementary monomeric reactant. The reactants diffuse to the interface, at which an interfacial polycondensation reaction produces the thin film, as shown schematically in Figure 1. The reaction is usually very fast and is quickly inhibited by the thin film that forms at the interface between the monomeric solutions. For commercial fabrication, a thick support layer (typically polysulfone) is soaked with an aqueous reactant solution and then brought into contact with an organic solution so that the permselective layer is formed directly on the support. The major advantages of the IP process include the lack of strict requirements for reactant purity and reagent stoichiometry, the formation of an ultrathin barrier layer (~0.1–0.25 μm), and the minimization of macrovoid defects.[1]

Despite a number of different IP chemistries, some general characteristics of the process can be inferred from the literature. In most IP systems, the interfacial reaction occurs on the organic side of the aqueous–organic interface, and so the film grows into the organic phase.[1] Arthur[2] studied the structure–property relationships in TFCs made by the IP reaction of trimesoyl chloride (TMC), cyclohexane-1,3,5-tricarbonyl chloride, and adamantane-2,6-dione-1,3,5,7-tetracarbonyl chloride with *m*-phenylene diamine (MPD) and found that the resulting permselective behavior de-

Correspondence to: V. P. Khare (khare@spot.colorado.edu).
Contract grant sponsor: NSF Industry/University Cooperative Research Center for Membrane Applied Science and Technology; contract grant number: EEC-0120725.

Journal of Applied Polymer Science, Vol. 90, 2618–2628 (2003)

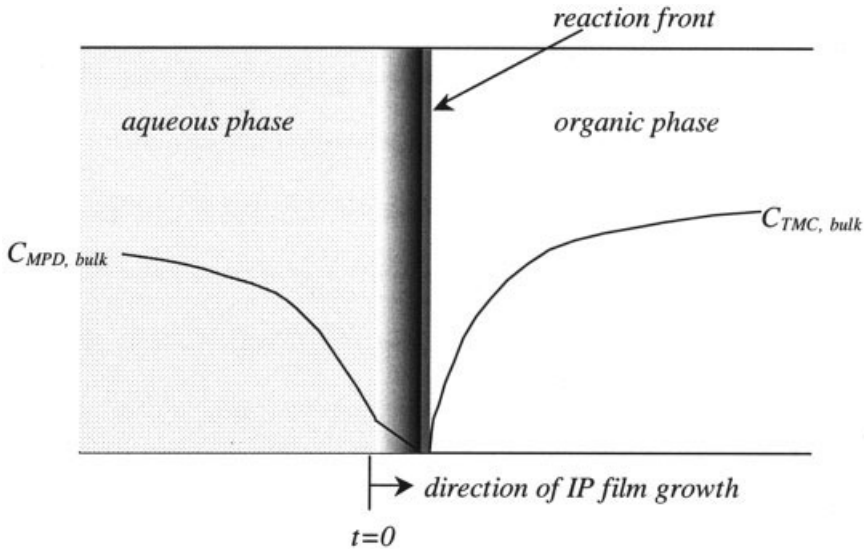

Figure 1 Schematic showing the IP-film formation for the MPD–TMC system. The film formation occurs on the organic side of the aqueous–organic interface; the MPD monomers have to diffuse through the already formed IP film to reach the reaction front.

pends on the extent of free volume and the conformational flexibility of the polymer chains. Jiang et al.[3] determined that in reverse osmosis (RO) and nanofiltration applications the solvent and solute fluxes depend on their interactions within the IP polymer network. Chen et al.[4] found that the addition of a swelling agent to a supporting microporous polysulfone membrane led to an increase in the TFC rejection for a diethylene triamine/terephthaloyl chloride system. Overall, these studies indicate that the structural characteristics of the barrier layer play an important role in membrane performance.

One of the most successful interfacially polymerized thin-film composite (IP-TFC) formulations was developed by Cadotte et al.;[5] it employs an interfacial reaction of MPD in the aqueous phase and TMC in the hexane organic phase (Fig. 2). The MPD monomer diffuses through the growing IP film and reacts with TMC on the organic side. The trifunctional nature of TMC enables the formation of a crosslinked polyamide; however, not all of the reacting trifunctional groups connect with adjacent ones to form crosslinks: some produce shorter unconnected segments of various lengths that result in dangling ends and branches. A byproduct of the reaction, HCl, is insoluble in the organic phase and diffuses back into the aqueous phase. Hydrolysis of the acyl chloride groups also occurs and gives the membrane a mildly acidic character.

Important information about the TMC–MPD system has been obtained from a few key experimental studies. Ko et al.[6] used electron spectroscopy for chemical analysis and determined that the ratio of branching to carboxyl group formation is 1:1. Cadotte et al.[5] reported that the trifunctional branching sites lead to the development of a three-dimensional polymeric network, which is insoluble in most common solvents, and Petersen[7] estimated that the average thickness of the IP barrier layer is approximately 2000 Å. Chai and Krantz[8] were the first to propose the use of pendant drop tensiometry to study IP-film formation in real time. They applied light reflectometry and pendant

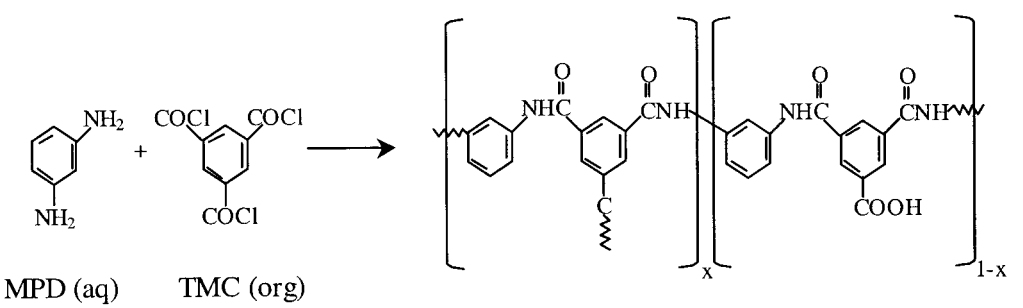

Figure 2 MPD–TMC reaction showing simultaneous side-chain formation (x) and hydrolysis leading to main-chain polymerization ($1 - x$). The pendant group in the side chains could result in crosslinking and branching.

drop tensiometry to monitor IP formation from TMC and MPD in real time and determined that the IP process is diffusion-controlled on the organic side under most formation conditions. Although reflectometry experiments imply that the time required for film formation varies from 5–70 s, pendant drop tensiometry results suggest that changes occur over timescales of up to 5 min, presumably because of the continuation of the crosslinking reaction.

Ji et al.[9] developed a rigorous mathematical model for the IP of 1,2-ethanediamine and disulfonyl chloride. Because the monomers are difunctional, only a linear polyamide would be formed. Therefore, such a model may not be appropriate for trifunctional or tetrafunctional monomers that lead to simultaneous crosslinking and branching during the IP-film formation. A later study by Ji et al.[10] reports a similar model for the formation of capsules with IP. However, the studied systems involve slow polymerization in which the IP-film formation typically occurs over 10–40 min. Therefore, the hydrodynamics of the film formation process may be fundamentally different from those encountered in MPD/TMC and similar IP-TFC systems.

Other experimental studies have used permeation and scanning electron microscopy methodologies employing the entire TFC.[11–13] Although these approaches provide useful information, they do not allow the specific contribution of the barrier layer to be assessed. A separate analysis of the barrier layer via conventional mass-based techniques is difficult given the relatively small mass of the ultrathin IP films. Moreover, an incomplete understanding of the relationship between the IP network structure and TFC performance has limited the potential for optimizing the properties of TFCs by the independent control of the properties of the different layers. Consequently, much of the current fabrication technology has developed through an extensive trial-and-error approach.

With this limitation in mind, we describe in this article a characterization methodology that can be applied to unsupported IP permselective films. The technique enables the measurement of the changes in the internal pressure and the size of an IP film that is formed on the surface of a pendant drop. The former permits stress–relaxation behavior to be assessed, whereas the latter can be directly related to the transport properties of the film. Of particular importance is that the information obtained from these studies provides important insights concerning the relationship between the IP network structure and performance. The subject methodology is based on the methodology first proposed by Greenberg et al.:[14] a pendant drop is pressurized at a constant rate until rupture so that the time-independent stress–strain behavior can be obtained. Roh et al.[15] recently used a variation of this pressure-to-rupture technique to characterize the rupture strength as a function of composition. As discussed in the following sections, this technique is more versatile and provides information about the IP-film network structure as well as the transport behavior of unsupported IP films.

TECHNIQUE DEVELOPMENT

Apparatus design

The pendant drop mechanical analysis (PDMA) technique is based on the principles of pendant drop tensiometry, which has been used to study a wide range of interfacial phenomena.[16–19] Modifications have been made to a commercially available pendant drop tensiometer (NRL C.A. 100-00-115 goniometer, Ramé-Hart, Inc., Mountain Lakes, NJ), and a schematic of the final pendant drop apparatus is shown in Figure 3. The IP reaction occurs when a drop of the aqueous phase suspended at the tip of a syringe is brought into contact with a surrounding organic phase (Fig. 1). The IP film then forms on the surface of the drop. The initial size of the drop is typically about 2 mm in diameter. Rapid contact between the two phases is achieved when a platform supporting a beaker of the organic phase is raised pneumatically by the activation of a solenoid valve, which allows high-pressure nitrogen gas to flow to the platform to provide a nearly instantaneous lift.

The volume of the liquid in the drop can be increased either by injection from the syringe or by transport from the surrounding fluid through the IP film. The mechanical experiments are based on measuring the internal pressure changes, whereas the transport experiments involve monitoring the increase in the drop size. Consequently, careful control of the injection rate and the ability to measure accurately any corresponding changes in the pressure and drop size are required. These critical design criteria are met as follows.

The syringe plunger is connected to a micrometer screw that is driven by a precision stepper motor. This arrangement allows control of the volumetric liquid injection rate into the drop. The stepper motor can drive the micrometer screw at five different speeds, which provide a volumetric injection rate range of 0.1–0.5 μL/s. A precision pressure transducer (163PC01D36, Omega, Stamford, CT) monitors the instantaneous internal pressure so that changes of 249 Pa (3.61×10^{-2} psi) can be resolved. The liquid injection rate and pressure data are stored on a laboratory computer.

A charge coupled device (CCD) camera is connected to a videocassette recorder that continuously records the drop images. A video board (Video Image 1200, Sun Valley, CA) in the computer then acquires the digital images at discrete time intervals from the vid-

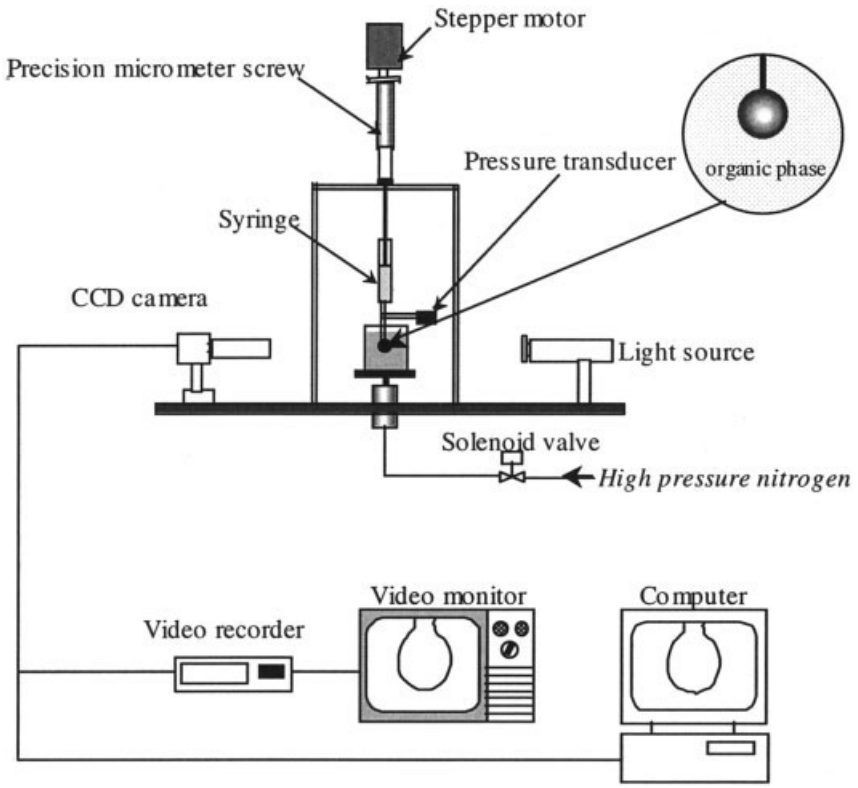

Figure 3 Schematic showing the main components of the PDMA apparatus used to study the viscoelastic (stress–relaxation) and transport (water-flux) properties of IP barrier layers.

eocassette recorder. The images store information in the form of grayscale values (520 pixels × 460 pixels). In this way, a spatial resolution of 10 μm is obtained. An in-house code has been developed that determines the drop profile from the drop images and calculates the instantaneous radius of curvature, surface area, and drop volume. The entire apparatus is supported on a vibration table to minimize disturbances.

Mechanical characterization

Two basic approaches can be employed to study the mechanical behavior of IP films. In a pressure-to-rupture experiment, an IP film at the surface of a drop is deformed by the injection of a liquid at a constant rate until drop rupture occurs. If the IP-film-drop configuration is represented as a spherical shell subjected to uniform internal pressure, then a biaxial stress state results in which the circumferential and tangential stresses are equal:

$$\sigma = \frac{Pr}{2t} \tag{1}$$

where P, r, and t are the internal gauge pressure, the radius of curvature, and the IP-film thickness, respectively. Although the instantaneous radius of curvature can be determined from the changes in the drop profile via the CCD camera, the instantaneous thickness cannot be easily measured. In addition, the corresponding values of strain will be proportional to the change in the instantaneous radius of curvature. Because stresses cannot be calculated without thickness values, plots of P versus Δr can be used to characterize the nondimensionalized stiffness, strength, and ductility of the IP films.[19] Although values of the parameters obtained with this approach have important limitations, they can provide useful information about trends in film behavior.[14]

Another approach to the mechanical characterization of IP films involves studying the stress–relaxation behavior. Given the nature of the *in situ* film-formation mechanism, in which polymerization and crosslinking occur simultaneously in the presence of the reactant solutions, a significant degree of viscoelastic response is expected. The protocol used was adopted after extensive preliminary experiments in which a liquid was injected into the IP-film-drop configuration until the drop internal pressure reached a predetermined value. Then, the pressure decay was followed as a function of time while the strain (radius) was maintained at a constant value. When the drop was exposed to air, the drop volume decreased with time because of the evaporation of water inside the drop. Consequently, the drop was immersed in pure heptane during liquid injection. A typical plot of the

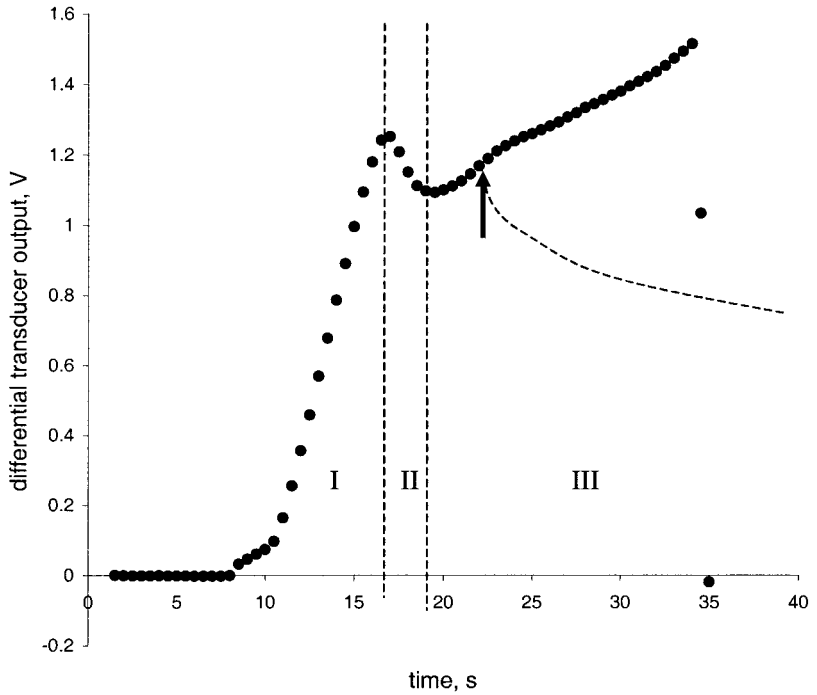

Figure 4 Representative plot showing the pressure–time response for a constant volumetric injection rate. The three behavior regions correspond to those described in the text. The arrow indicates the starting point for the stress–relaxation experiments, and the pressure profile follows the path represented by the dashed line.

pressure injection versus time is shown in Figure 4, in which three distinct regions can be characterized. The pressure increases at a relatively high rate in region I, decreases for a small time in region II, and increases again in region III at a lower rate than in region I. Visual observations of the IP-film deformation reveal that in region I, the injected liquid fills up the creases and folds in the IP film; as these creases pop open, additional volume is created that leads to the decrease in pressure observed in region II. Measurements of the drop profile indicate that deformation of the overall film occurs only in region III. Therefore, all stress–relaxation experiments were conducted at initial pressure values corresponding to region III. The dashed line in Figure 4 indicates a typical pressure profile when injection was ceased at the arrow (instead of liquid injection continuing until IP-film rupture) and the IP-film relaxation was monitored. A typical relaxation curve is shown in Figure 5 in which the normalized pressure (instantaneous pressure divided by the

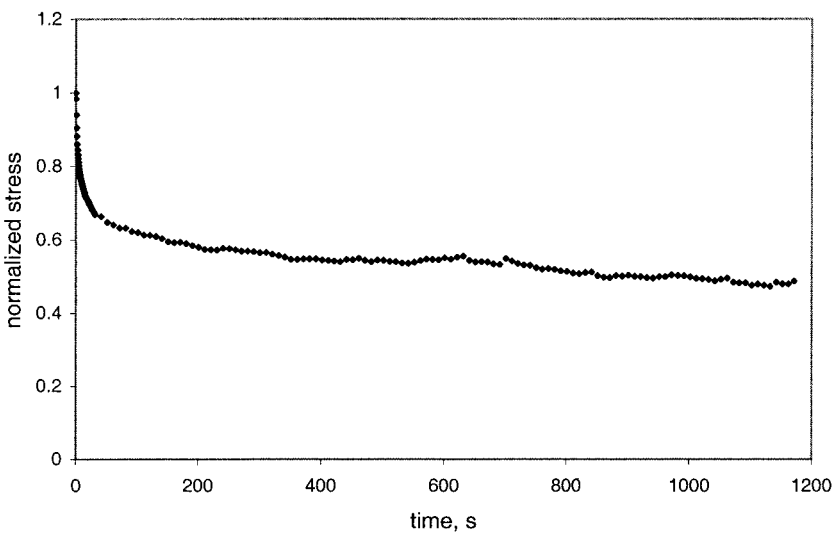

Figure 5 Representative results from a stress–relaxation experiment conducted on an IP-film-covered pendant drop. The drop dimensions remain constant over the experimental 1200-s timescale.

initial pressure, P/P_0) is plotted as a function of time. The normalized pressure will be equal to the normalized stress (σ^*) via eq. (1) and obviates the need to determine the initial *in situ* film thickness. An independent measurement of the drop profile during the relaxation confirmed that the drop size (radius) remained constant for the duration of the test.

To describe the stress–relaxation behavior, we have used the fractional exponential relaxation model, which is based on the Williams–Watts equation.[20] The latter is a two-parameter empirical relationship originally proposed to describe the dielectric relaxation of amorphous polymers.[21] This equation relates the instantaneous stress [$\sigma(t)$] to time t via two parameters (τ and β) and the initial stress (σ_0):

$$\sigma(t) = \sigma_0 \exp\left[-\left(\frac{t}{\tau}\right)^{\beta}\right] \tag{2a}$$

τ is the characteristic relaxation time and is close to, but not necessarily at, the peak of the corresponding continuous relaxation spectrum.[22,23] The exponent β varies between 0 and 1 and describes the intensity distribution or spread of the relaxation spectrum. This model has been successfully applied to mechanical relaxation phenomena in polymers in their glassy state.[24,25]

The fractional exponential relaxation model is a more generalized form of the Williams–Watts equation and is used when the polymer shows an equilibrium relaxation value:

$$\sigma(t) = \sigma_e + (\sigma_0 - \sigma_e) \exp\left[-\left(\frac{t}{\tau}\right)^{\beta}\right] \tag{2b}$$

where σ_e is the equilibrium stress–relaxation value. Because the polyamide tested in this work was a crosslinked polyamide, it was quite likely that the polymer would show a finite equilibrium relaxation. The measurement of this equilibrium value would have necessitated running the relaxation experiments for a long time. However, over such long times, heptane evaporation would become significant and affect the pressure measurement. Moreover, such long-time experiments would significantly limit the number of repeats, as well as the number of different measurements, that we could perform in a reasonable time. Because of these considerations, we decided to perform short-time experiments in which, for each run, stress relaxation was measured for 1200 s (20 min) only. For all the cases tested, no equilibrium relaxation was observed; that is, σ^* had not attained any asymptotic value at the end of 1200 s. Therefore, in this time frame, the stress–relaxation data were fit to the two-parameter Williams–Watts equation.

Because of the uncertainty concerning the thickness of the IP films, eq. (2a) was normalized with

$$\sigma^* = \frac{\sigma(t)}{\sigma_0} = \frac{P(t)}{P_0} \tag{3}$$

In this way, σ^* is given by the ratio of the instantaneous pressure to the initial injection pressure as long as the stress is directly proportional to the pressure via a relationship similar to eq. (1). The values of τ and β were obtained from plots of σ^* versus t with a nonlinear least-squares algorithm to provide the best fit.[26]

Transport characterization

In addition to mechanical characterization, the pendant drop configuration also enables the study of the transport behavior of the barrier layer independent of any support. Water transport through the IP film is achieved by the establishment of an osmotic pressure gradient via the inclusion of 0.5 wt % NaCl in the aqueous solution used to form the pendant drop before film formation. After the polymerization, the film-covered drop is immersed in deionized water. The difference in the NaCl concentrations causes water to move through the film from the surroundings, and so the drop becomes larger. The rate at which this occurs can be determined from CCD camera measurements of the drop profile as a function of time. The transport properties of the IP film can be represented in terms of a membrane constant (A) and related to the changes in the drop profile by means of a simple model.

According to the classical solution-diffusion model, the water flux (J_{water}) is given by

$$J_{\text{water}} = \rho A(\Delta P - \Delta\pi) \tag{4}$$

where ρ is the solution density, ΔP is the transmembrane pressure difference, and $\Delta\pi$ is the transmembrane osmotic pressure difference. A is a lumped parameter that combines the contributions of the solvent diffusivity through the IP film, the solvent activity, and the IP-film thickness. A is proportional to the IP-film permeability (a material property) and inversely proportional to its thickness (a geometric parameter). The osmotic pressure depends on the concentration of the solute in the solution; for relatively small concentrations, it is a linear function of the solute concentration.

Because the transport of water occurs only because of the osmotic pressure gradient, ΔP is zero, and J_{water} can be expressed as follows:

$$J_{\text{water}} = \rho A k C_m \tag{5}$$

where C_m is the local concentration of NaCl inside the drop adjacent to the IP film and k is the constant that relates the osmotic pressure to the NaCl concentration. C_m will be equal to the bulk concentration (C_{bulk}) in the drop only if the resistance to diffusion (R_1) of water in the NaCl solution inside the drop is low compared with the resistance to the diffusion of water through the IP film (R_2). An analysis of the timescales for the diffusion of water through the NaCl solution and the IP film has revealed that the timescale of the former is much greater than that of the latter. Therefore, C_m cannot be taken as equal to C_{bulk}. One method of modeling the instantaneous water flux would be to solve the comprehensive diffusion equations for water diffusion inside the drop, across the IP film, and in the outer liquid and to couple these with appropriate boundary conditions. However, the diffusive flux of water into the drop can be obtained more simply if R_1 and R_2 are accurately modeled. Because the liquid inside the drop is quiescent, water transport occurs purely by diffusion. Therefore, R_1 can be determined reasonably well with the Higbie penetration theory:

$$R_1 = \sqrt{\frac{\pi t}{D}} \tag{6}$$

where D is the diffusion coefficient of water in a water–NaCl mixture ($D = 2.2 \times 10^{-5}$ cm^2/s at 25°C[27]) and t is the time. R_2 can be obtained from eqs. (4) and (5) as follows:

$$R_2 = \frac{1}{\rho A k} \tag{7}$$

Therefore, the flux of water inside the drop can be determined from eqs. (5)–(7):

$$J_{\text{water}} = \frac{C_{\text{bulk}}}{\sqrt{\frac{\pi t}{D}} + \frac{1}{\rho A k}} \tag{8}$$

Rewriting this equation in a simple form with constants k_1 and k_2 leads to

$$J_{\text{water}} = \frac{C_{\text{bulk}}}{k_1\sqrt{t} + k_2} \text{ where } k_1 = \sqrt{\frac{\pi}{D}} \text{ and } k_2 = \frac{1}{\rho A k} \tag{9}$$

If V is the instantaneous drop volume, then,

$$\frac{dV}{dt} = 4\pi r^2\left(\frac{1}{\rho}\right)\frac{C_{\text{bulk}}}{k_1\sqrt{t} + k_2} \tag{10}$$

If the volume is expressed in terms of the radius of curvature of the drop, and eq. (10) is integrated from the initial time ($t = 0$), the following relationship is obtained:

$$\frac{r}{r_0} = 1 + \frac{2C_{\text{bulk}}}{\rho k_1^2 r_0}\left\{k_1\sqrt{t} - k_2 \ln\left[\frac{k_1\sqrt{t}+k_2}{k_2}\right]\right\} \tag{11}$$

Now k_2 and, therefore, A can be obtained from a regression analysis on a plot of r/r_0 versus the square root of time. The regression algorithm, based on an iterative technique, is described in detail in ref. 26.

EXPERIMENTAL

IP-film preparation

The MPD–TMC system was chosen for these studies because the properties of this system have been relatively well documented in the open literature. Solutions of the two IP reactants were prepared by the mixing of MPD (Aldrich Chemical, Milwaukee, WI) in deionized and distilled water and TMC (Aldrich Chemical) in reagent-grade heptane. Although hexane is used as the organic solvent in commercial formulations of this system, heptane was chosen for these experiments because its lower volatility makes it more amenable to pendant drop procedures. With the modified pendant drop apparatus previously described, polymerizations were conducted for 1 min at 23°C with a fixed concentration of MPD (2 wt %) and TMC concentrations ranging from 0.05 to 0.5 wt %. At the completion of the contact period, the TMC–heptane solution surrounding the drop was immediately exchanged for one containing pure heptane so that any excess TMC was removed from the IP-film surface; this was followed by a 1-min exposure to ambient air to allow any remaining heptane to evaporate. This protocol prevented a continued reaction by excess TMC during the subsequent mechanical and transport experiments.

IP-film characterization

The stress–relaxation experiments were performed over a 20-min period after the drop was initially pressurized to provide a small uniform deformation corresponding to a position within stage III (Fig. 4, arrow). The timescale of the relaxation experiments was short enough to ensure that the assumption of a constant strain was valid. The water transport experiments were conducted over a timescale of 30 min. Over this period, the drop size increased by at least 30%, whereas the NaCl concentration in the external water remained negligible. The 0.5 wt % NaCl added to the MPD–water solution for the water permeation experiments did not appear to have any significant effect on the MPD–TMC reaction according to comparative stress–relaxation experiments.

TABLE I
Effect of TMC Concentration on τ and β of the Williams–Watts equation, σ^*_{1200}, and A

TMC concentration (wt %)	τ (s)[a]	β[b]	σ^*_{1200}	$A \times 10^8$ (m/s bar)[c]
0.01	928 ± 134 (5)[d]	0.264 ± 0.034 (5)	0.341 ± 0.012	4.26 ± 0.53 (3)
0.03	1057 ± 152 (4)	0.271 ± 0.027 (4)	0.357 ± 0.014	
0.05	1697 ± 677 (4)	0.256 ± 0.010 (4)	0.397 ± 0.042	4.00 ± 0.47 (3)
0.08	3328 ± 236 (4)	0.249 ± 0.021 (4)	0.463 ± 0.013	
0.1	5029 ± 1148 (5)	0.234 ± 0.015 (5)	0.511 ± 0.014	4.11 ± 0.28 (4)
0.3	4719 ± 245 (5)	0.226 ± 0.008 (5)	0.484 ± 0.007	2.72 ± 0.25 (3)
0.5	1834 ± 129 (4)	0.219 ± 0.005 (4)	0.406 ± 0.005	2.33 ± 0.80 (3)
0.8	2069 ± 204 (4)	0.224 ± 0.014 (4)	0.408 ± 0.007	

[a] τ versus TMC was statistically significant with $p < 0.001$ (Krushkal–Wallis test).
[b] β versus TMC was statistically significant with $p < 0.005$ (one-way ANOVA).
[c] A versus TMC was statistically significant with $p < 0.005$ (one-way ANOVA).
[d] The number of replicates is in parentheses.

Experimental design and statistical analysis

For each of the PDMA experiments, a single-factor factorial design with replication was used. The statistical significance of the results was determined with a one-way analysis of variance (ANOVA) followed by a Tukey test to identify which levels were statistically different. If the normality assumptions required for ANOVA could not be met (one case), a nonparametric technique, the Krushkal–Wallis test, was used. In this case, pairwise multiple comparisons were made with Dunn's method. In all cases, the statistical significance was defined in terms of a probability of 5% or less, that is, $p \leq 0.05$ (Table I).

RESULTS AND DISCUSSION

Although many studies have confirmed that modifications in structure, as manifested through changes in the molecular weight, crosslinking, and branching, can alter the stress–relaxation response of polymers, establishing a general physical significance for the empirical parameters τ and β is difficult.[28] In fact, a combination of different factors, including the molecular weight distribution, the presence and weight distribution of crosslinks, the crosslink polyfunctionality, and the presence of entanglements, could all lead to similar values of τ and β. Therefore, to interpret τ and β values for this specific study, one needs to consider the most probable mechanisms for stress relaxation in the MPD–TMC polyamide system. In this context, the research of Aharoni and coworkers[29–31] provides valuable insights. Their research focused on understanding the evolution of three-dimensional crosslinked polyamide structures from multifunctional monomers via *in situ* condensation polymerization. Aharoni and coworkers proposed that in the *in situ* polyamidation reactions, a relatively small number of highly branched, high-molecular-weight macromolecules are formed, and the reaction mixture contains a changing distribution of lower molecular weight macromolecules extending to monomeric size. The molecular weight and molecular weight distribution of the macromolecules change during the condensation reaction, and this results in a polymeric network encompassing the whole reaction volume, within which are interpenetrated and in whose voids and irregular surfaces are nestled other macromolecules of lower molecular weight. According to these researchers, the initiation of the structure is through the formation of random nucleation that forms polymer fractals. These fractals cluster together, and when a sufficient number of them grow large, a contiguous network is formed. Such networks, which the researchers termed *fractal polymers*, are intrinsically different from conventional crosslinked networks, in which crosslinks are introduced between linear chains.

For the TMC–MPD system, two factors, the ratio and the magnitude of the instantaneous monomer fluxes to the reaction front, play a pivotal role in determining the crosslinking density of the eventual network. For example, if the flux of the TMC monomers is much higher than that of the MPD monomers, individual MPD monomers will be surrounded by the TMC monomers, and this will form a seed nucleus with four functional groups. In contrast, if the instantaneous flux of the MPD monomers is much higher, the individual TMC monomers will be surrounded by the MPD monomers, and the seed nucleus will have three functional groups. Although the monomer flux ratio determines the fractal dimensionality, the monomer flux magnitude determines the number density of the nuclei. Very low monomer fluxes result in relatively fewer nuclei in a given volume. Their fractal growth will occur to a greater extent before they begin to interact with one another. In contrast, when the fluxes are higher, a greater number of nuclei will be formed, and interactions between the nuclei will occur before a similar extent of fractal growth occurs. The continuous network formed under the latter condi-

tions will be restricted and have greater degrees of crosslinking than the former. The exact relationship between the crosslink density and the monomer concentrations is, therefore, very complicated, but it is conceivable that a particular combination of the MPD and TMC concentrations will lead to a maximum in the crosslinking density.

Because the IP polyamide network has a wide distribution in the molecular weights of the linear chains and any pendant chains, a distribution in the relaxation time spectrum is expected because each of the chains and branches has a different value of τ. τ is generally associated with the structural rigidity.[32,33] In this specific context, we believe that τ indicates the relative degree of crosslinking. Likewise, because β is related to the broadness of the relaxation-time spectrum,[32] in this case we believe that β indicates the polydispersity in the linear chain segments and the degree of branching.

The general characteristics of the stress–relaxation curves obtained in this study are represented by the data shown in Figure 5. A relatively rapid decrease in σ^* over the first 50 s is followed by a more gradual decrease over the remaining experimental timescale. Ideally, the stress–relaxation experiments would be continued for a much longer time, and this would establish whether an equilibrium stress was achieved (indicating a crosslinked network) or whether complete stress relaxation occurred. However, experimental limitations constrained us to measurements for only 20 min; at longer times, heptane evaporation became significant and affected the pressure readings. Significantly, even the relatively short-time measurements were adequate for distinguishing among the barrier layers made from different MPD/TMC concentrations. An analysis of the PDMA relaxation data indicate that the slope of the relaxation curves becomes less negative as the TMC concentration increases from 0.01 to 0.1 wt %. In addition, the normalized stress at the end of 20 min (σ^*_{1200}; Table I) increases over this composition range by about 50%. Therefore, the observed trend suggests an increased degree of crosslinking with increasing TMC concentration up to 0.1 wt %. In contrast, over the range of 0.1–0.8 wt % TMC, these trends are reversed with a corresponding decrease in τ.

The experimental results for τ and β are summarized in Table I as a function of the TMC concentration for IP-film-covered drops prepared with 2 wt % MPD and a contact time of 1 min. The mean values of each parameter are based on a minimum of three independent runs; given the relatively small sample size, the variability in most cases is modest. Statistical analysis (Table I) indicates that differences among the τ values are highly significant ($p < 0.001$). In addition, the results show that the values of τ at TMC concentrations of 0.1 and 0.3 wt % are higher than the values at

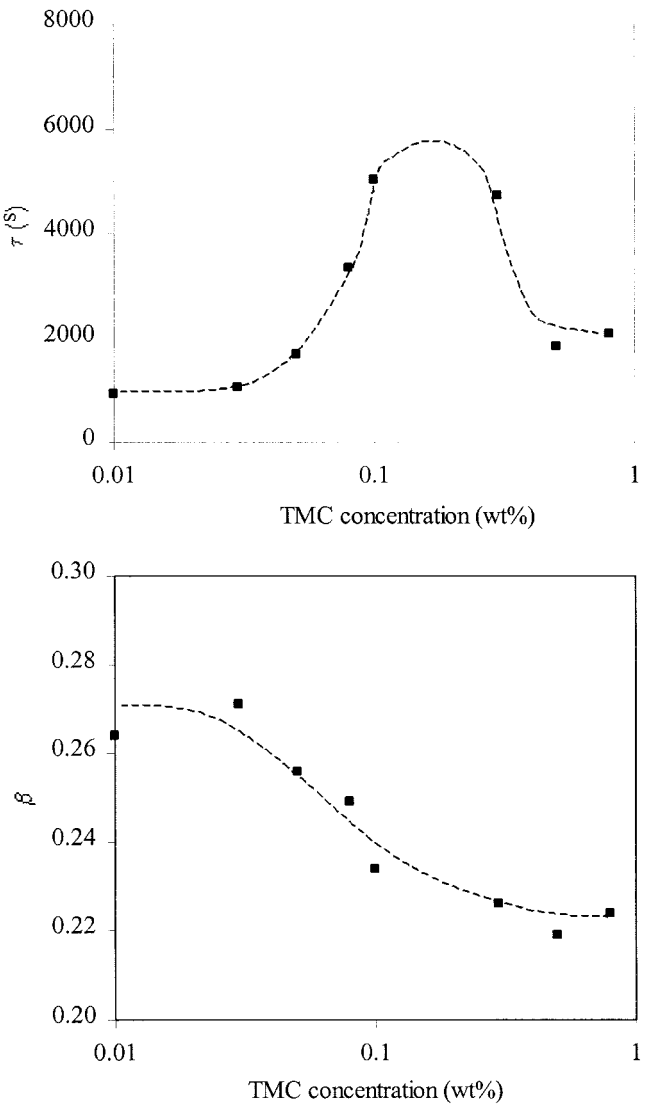

Figure 6 Dependence of the Williams–Watts relaxation model parameters τ and β on the TMC concentration. The curves are estimated from a statistical analysis of the results and indicate the general trend.

the other concentrations. The mean values of τ are plotted as a function of composition in Figure 6, with consideration given to the statistical findings. Although the results indicate that τ reaches a maximum between 0.1 and 0.3 wt % TMC, the true maximum may well occur at a TMC concentration different from the value of 0.15 wt % shown in Figure 6.

An analysis of the data also indicates a statistically significant dependence of β on the TMC concentration (Table I), with β values at the higher TMC concentrations (0.3, 0.5, and 0.8 wt %) being smaller than those at the lower TMC concentrations (0.01 and 0.03 wt %). In light of the previous discussion, this implies a consistently increasing polydispersity of linear chains and degree of branching. To our knowledge, this research is the first demonstration in the open literature of the

dependence of the network characteristics on the IP formation systems.

The values of A determined via PDMA experiments are also given in Table I. Compared to the values reported in the open literature,[34] the measured A values are about an order of magnitude smaller (61.1–64.8 $\times 10^{-8}$ m/s bar). A number of major differences between the transport measurements via PDMA and those made in a conventional RO setup could account for this discrepancy. In our setup, the barrier layers are unsupported. Therefore, we could not apply the usually high (4.0–5.6 MPa) RO pressures. Water transport in PDMA was achieved via an osmotic pressure difference and occurred from the organic side of the barrier layer to its aqueous side. Conventional RO measurements are carried out on the entire TFC membrane, and the water transport occurs from the aqueous side of the barrier layer to its organic side. Another major difference is in the state of the barrier layer. The *in situ* network made from the condensation reaction of MPD and TMC is highly amorphous and most likely swollen by the organic solvent. Indeed, the preliminary cryo-scanning electron microscopy measurements that we performed on the as-formed barrier layers seemed to indicate that their thickness was much larger, around 1 μm. In contrast, in the IP-TFC membrane, the barrier layer is not swollen and is, therefore, much thinner ($\sim$0.1 μm).[7] An additional aspect that has to be considered is that commercial membranes are subjected to posttreatment, which also enhances the membrane flux.

Despite the major differences highlighted, we believe that PDMA measurements are still very valuable because they reveal information about the barrier layer alone. Therefore, any differences in J_{water} will only be due to the differences in the network structure of the barrier layer. The results indicate that A decreases by approximately 35% when the TMC concentration is increased from 0.1 to 0.3 wt % (Fig. 7). An analysis has confirmed that the change in A between 0.1 and 0.3 wt % is statistically significant and corresponds to the same composition range over which τ most likely attains a maximum value. Whereas prior studies have demonstrated a generally inverse relationship between the permeability and the extent of crosslinking,[35] the specific correspondence between a crosslinking maximum (as indicated by τ) and a relatively abrupt decrease in the permeation rate has not been previously reported for the MPD–TMC system. Interestingly, a trial-and-error approach has established that the optimum performance for commercial membranes with the TMC–MPD system also lies within the range of 0.1–0.3 wt % TMC. Although these results are encouraging and suggest that the PDMA technique can be used to establish an ideal composition range, additional studies are required to validate this outcome.

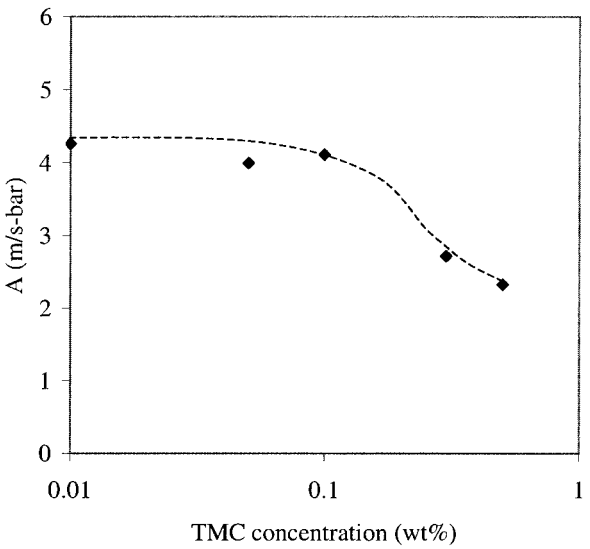

Figure 7 Dependence of A on the TMC concentration. The curve is estimated from a statistical analysis of the results and indicates the general trend.

CONCLUSIONS

The nature of the relationship between the structure and performance of IP barrier layers has not previously been considered in detail because of the difficulty in determining the behavior of unsupported thin films. The subject experiments of the TMC–MPD system demonstrate that this limitation can be effectively addressed via the PDMA technique. Specifically, this study has shown that the mechanical behavior of IP-film-covered drops can be well described by the Williams–Watts equation. The τ and β parameters of this relaxation model depend on the TMC concentration such that a maximum in τ and a decrease in β occur in a concentration range between 0.1 and 0.3 wt %. These results may be consistent with enhanced network formation in this concentration range. Moreover, permeation experiments indicate that values of A are also dependent on the TMC concentration, and so a significant decrease in A occurs in the concentration range over which τ reaches a maximum. These findings provide important information regarding the relationship between structure and performance in an unsupported IP film.

Despite this initial success, the PDMA technique requires additional refinement so that IP-film-covered drops are more uniformly robust. Acceptable levels of reproducibility in the mechanical and transport properties require great care in the IP-film-formation portion of the protocol. Nonetheless, the PDMA technique offers a means by which extensive large-scale trial-and-error experimentation can be reduced so that optimum combinations of process variables can be obtained more efficiently. In addition, the ability to isolate the dense layer may provide an effective means

of studying other IP phenomena such as the mechanism of chlorine attack on polyamide thin films.

The authors also thank Norm Taylor and Willy Groethe for their help in fabricating the PDMA apparatus and Kenneth Stuttz and Richard Fibiger from Dow Chemical Co. for their helpful comments and suggestions.

References

1. Morgan, J. P. Condensation Polymers; Interscience: New York, 1965.
2. Arthur, S. D. J Membr Sci 1989, 46, 243.
3. Jiang, J.; Mingji, S.; Minling, F.; Jiayan, C. Desalination 1989, 71, 107.
4. Chen, S.; Chang, D.; Liou, R.; Hsu, C.; Lin, S. J Appl Polym Sci 2002, 83, 1112.
5. Cadotte, J. E.; Petersen, R. J.; Larson, R. E.; Erickson, E. E. Desalination 1980, 32, 25.
6. Ko, J.; Petersen, R. J.; Cadotte, J. E. Polym Prepr (Am Chem Soc Div Polym Sci) 1986, 27, 391.
7. Petersen, R. J. J Membr Sci 1993, 83, 81.
8. Chai, G. Y.; Krantz, W. B. J Membr Sci 1994, 93, 175.
9. Ji, J.; Dickson, J. M.; Childs, R. F.; McCarry, B. E. Macromolecules 2000, 33, 624.
10. Ji, J.; Childs, R. F.; Mehta, M. J Membr Sci 2001, 192, 55.
11. Mehdizadeh, H.; Dickson, J. M. Ind Eng Chem Res 1989, 28, 814.
12. Mukherjee, D.; Kulkarni, A.; Gill, W. N. J Membr Sci 1994, 97, 231.
13. Lipp, P.; Gimbel, R.; Frimmel, F. H. J Membr Sci 1994, 95, 185.
14. Greenberg, A. R.; Khare, V. P.; Krantz, W. B. Mater Res Soc Symp Proc 1995, 356, 541.
15. Roh, I. J.; Kim, J.; Park, S. Y. J Membr Sci 2002, 197, 199.
16. Thiessen, D. B.; Chione, D. J.; McCreary, C. B.; Krantz, W. B. J Colloid Interface Sci 1996, 177, 658.
17. Van Hunsel, J.; Bleys, G.; Joos, P. J Colloid Interface Sci 1986, 114, 432.
18. Bain, C. D.; Whitesides, G. M. Langmuir 1989, 5, 1370.
19. Zhang, W.; Hallstrom, B. Desalination 1990, 79, 1.
20. Williams, G.; Watts, D. C. Trans Faraday Soc 1970, 66, 80.
21. Ho, T.; Mijovic, J.; Lee, C. Polymer 1991, 32, 619.
22. Povolo, F.; Hermida, E. B. Mech Mater 1991, 12, 35.
23. Povolo, F.; Hermida, E. B. Phys Status Solidi B 1995, 192, 53.
24. Ngai, K. L.; Fytas, G. J Polym Sci Part B: Polym Phys 1986, 24, 1683.
25. Stastna, J.; DeKee, D.; Powley, M.; Schummer, P.; Otten, B. J Rheol 1989, 33, 1157.
26. Khare, V. P. Ph.D. Thesis, University of Colorado at Boulder, 1996.
27. McCall, D. W.; Douglas, D. C.; Anderson, E. W. J Chem Phys 1959, 31, 1555.
28. Ferry, J. D. Viscoelastic Properties of Polymers, 3rd ed.; Wiley: New York, 1980.
29. Aharoni, S. M.; Murthy, N. S.; Zero, K.; Edwards, S. F. Macromolecules 1990, 23, 2533.
30. Aharoni, S. M.; Edwards, S. F. Macromolecules 1989, 22, 3361.
31. Aharoni, S. M. Macromolecules 1991, 24, 235.
32. Matsuoka, S. Relaxation Phenomena in Polymers; Hanser: New York, 1992.
33. Hermida, E. B. Phys Status Solidi B 1993, 178, 311.
34. Rautenbach, R.; Albrecht, R. Membrane Processes; Wiley: New York, 1989.
35. Oikawa, E.; Hibi, K.; Sakazume, N.; Endo, H.; Honda, T.; Aoki, T. Desalination 1993, 94, 25.